Inorganic Chemistry

Article

pubs.acs.org/IC

Cobalt Porphyrin–Polypyridyl Surface Coatings for Photoelectrosynthetic Hydrogen Production

A. M. Beiler, D. Khusnutdinova, B. L. Wadsworth, and G. F. Moore*

School of Molecular Sciences and the Biodesign Institute Center for Applied Structural Discovery (CASD), Arizona State University, Tempe, Arizona 85287-1604, United States

Supporting Information

ABSTRACT: Hybrid materials that link light capture and conversion technologies with the ability to drive reductive chemical transformations are attractive as components in photoelectrosynthetic cells. We show that thin-film polypyridine surface coatings provide a molecular interface to assemble cobalt porphyrin catalysts for hydrogen evolution onto a visible-light-absorbing p-type gallium phosphide semiconductor. Spectroscopic techniques, including grazing angle attenuated total reflection Fourier transform infrared spectroscopy, confirm that the cobalt centers of the porphyrin macrocycles coordinate to pyridyl nitrogen sites of the organic surface coating. The cobalt porphyrin surface concentration and fraction of pyridyl sites coordinated to a cobalt center are quantified using complementary methods of ellipsometry, inductively coupled plasma mass spectrometry, and X-ray photoelectron spectroscopy. In aqueous solutions under simulated solar illumination the modified cathode is photochemically active for hydrogen production, generating the product gas with near-unity Faradaic efficiency at a rate of ≈10 μL min^{-1} cm^{-2} when studied in a three-electrode configuration and polarized at the equilibrium potential of the H^+/H_2 couple. This equates to a photoelectrochemical hydrogen evolution reaction activity of 17.6 H_2 molecules s^{-1} Co^{-1}, the highest value reported to date for a molecular-modified semiconductor. Key features of the functionalized photocathode include (1) the relative ease of synthetic preparation made possible by application of an organic surface coating that provides molecular recognition sites for immobilizing the cobalt porphyrin complexes at the semiconductor surface and (2) the use of visible light to drive cathodic fuel-forming reactions in aqueous solutions with no added organic acids or sacrificial chemical reductants.

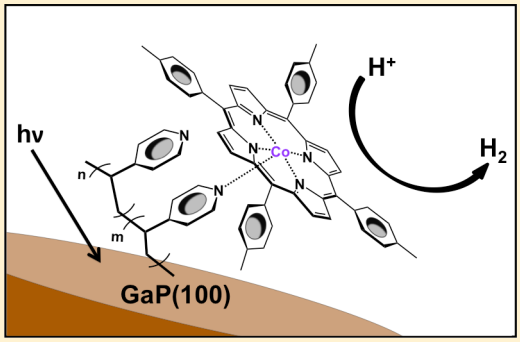

INTRODUCTION

Future clean energy scenarios require development of effective methods for converting and storing intermittent energy sources.[1] In this context, the photoelectrochemical (PEC) production of fuels using sunlight as an energy input has emerged as a promising storage option that could be integrated with our existing petroleum-based infrastructure.[2] An active area of research in the field of solar fuels focuses on strategies to interface light capture and conversion technologies with appropriate electrocatalysts for generating fuels and industrially relevant chemical feedstocks.[3] However, this approach is constrained by the use of precious metal catalysts or relatively high energy inputs.[4]

In biological catalysis, enzymes use soft material interactions, including coordination to amino acid residues along a protein scaffold, to provide appropriate three-dimensional environments for controlling the catalytic activity and selectivity of metal centers composed of earth-abundant elements.[5] In a similar vein, a focus on the role of secondary coordination sphere interactions has emerged as a bioinspired design theme in synthetic molecular catalysis, providing improved routes for binding substrates, lowering transition state energies along a reaction coordinate, and releasing products.[6]

Herein, we report the use of a surface-grafted organic coating to assemble molecular catalysts for hydrogen evolution to a visible-light-absorbing semiconductor. This approach combines features of solid-state light capture and conversion materials with molecular components for enhancing photoelectrochemical fuel production. The materials used to assemble the hybrid photocathode include gallium phosphide (GaP) as the underpinning semiconductor support, 4-vinylpyridine as the monomeric unit used to form a polypyridine surface coating (PPy), and 5,10,15,20-tetra-*p*-tolylporphyrin cobalt(II) (CoTTP) as a molecular component for enhancing photoelectrochemical hydrogen production.

GaP is a III–V semiconductor with an indirect band gap of 2.26 eV. The energetic positioning of the conduction band (≈−1 V vs normal hydrogen electrode (NHE)) more than satisfies the thermodynamic requirement for driving the hydrogen evolution reaction (HER), prompting researchers to investigate this material for PEC applications since the 1970s.[7] However, its performance is limited by photocorrosion in aqueous conditions and surface defect sites that hinder

Received: June 15, 2017
Published: October 3, 2017

ACS Publications © 2017 American Chemical Society

DOI: 10.1021/acs.inorgchem.7b01509
Inorg. Chem. 2017, 56, 12178–12185

efficient transfer of photogenerated minority carriers at the semiconductor|liquid junction.[7e] Molecular modification of semiconductors, including GaP, has been used as a strategy to confer chemical stability to surfaces, provide nanoscale control over interface properties, and improve rates of PEC fuel production.[8] Although some progress has been made in development of such assemblies, finding new and more effective ways to interface molecular components to semiconductor surfaces remains a major challenge.[4a] In this report, GaP(100) substrates serve as commercially available materials for developing a metalloporphyrin attachment chemistry that will likely be extensible to other semiconductor crystal faces[8e] as well as conductive oxide-terminated surfaces.[8d]

Metalloporphyrins serve important roles in biology as reactive sites for driving enzymatic reactions and as components in emerging molecular-based materials with applications to energy transduction.[9] As electrocatalysts, they are capable of chemically transforming protons into hydrogen as well as converting carbon dioxide into carbon monoxide and/or hydrocarbons such as methane and ethylene when electrochemically activated in solution or immobilized at a conductive substrate polarized at an appropriate potential. We have previously reported a synthetic methodology for directly grafting metalloporphyrins onto GaP using precursor complexes bearing a 4-vinylphenyl surface attachment group at the beta position of the porphyrin macrocycle.[8c] The cobalt porphyrin modified photocathodes are active for hydrogen production, evolving the product gas at a rate of ≈10 μL min^{-1} cm^{-2}. Comparison of the total surface cobalt porphyrin concentrations with the amount of hydrogen produced indicates that the HER activity per metal site is among the highest reported for a molecular-modified semiconductor photocathode operating at the H^+/H_2 equilibrium potential under 1-sun illumination.

We now show that an initially deposited organic interface consisting of repeating pyridyl units can provide molecular recognition sites that self-assemble cobalt porphyrins onto the polypyridine-modified GaP surface. This provides an alternate and streamlined method for interfacing cobalt porphyrins to a semiconductor that does not require synthetic modifications to the porphyrin macrocycle to install a surface-grafting functional group. Thus, the attachment strategy also enables application of porphyrins bearing substituents that are chemically incompatible or complicated by installment of the vinylphenyl functionality.

EXPERIMENTAL SECTION

Materials. All reagents were purchased from Sigma-Aldrich. Dichloromethane, hexanes, methanol, and toluene were freshly distilled before use. Milli-Q water (18.2 MΩ·cm) was used to prepare all aqueous solutions. Single crystalline p-type Zn-doped gallium phosphide (100) wafers (University Wafers) were single side polished to an epi-ready finish. The GaP(100) wafers have a resistivity of 0.16 Ω·cm, a mobility of 69 cm^2 V^{-1} s^{-1}, and a carrier concentration of 4.5 × 10^{17} cm^{-3}, with an etch pit density of less than 5 × 10^4 cm^{-2}.

Synthesis. The compounds 5,10,15,20-tetra-*p*-tolylporphyrin (TTP) and 5,10,15,20-tetra-*p*-tolylporphyrin cobalt(II) (CoTTP) were synthesized using modified versions of previously reported procedures.[10] Further details are available as Supporting Information.

Wafer Preparation. The use of 4-vinylpyridine as a precursor for surface functionalization of GaP has been previously reported.[8e,f,q,r,s] Briefly, diced semiconductor samples were etched with buffered hydrofluoric acid before exposure to an argon-sparged solution of the neat monomer 4-vinylpyridine under 254 nm UV light for 2 h (see the Supporting Information for details). The PPy-functionalized samples were then soaked for 18 h in a CoTTP solution (1 mM) in toluene.

Wafer Characterization. Surface characterization of the wafers was carried out using ellipsometry, grazing angle attenuated total reflection Fourier transform infrared spectroscopy (GATR-FTIR), X-ray photoelectron (XP) spectroscopy, and inductively coupled plasma mass spectrometry (ICP-MS) (see the Supporting Information for details).

Loading Efficiency. The reported cobalt surface concentration takes into account that the synthetic method (UV-induced grafting of 4-vinylpyridine followed by wet chemical treatment with a CoTTP solution) and the reaction vessel geometry used in this report yield samples with cobalt porphyrin assembled on both sides of the single side polished GaP wafers. The total cobalt, including contributions from the front and back sides of the GaP wafer and as measured by ICP-MS following acid digestion of CoTTP|PPy|GaP samples, is 0.59 ± 0.12 nmol cm^{-2}. Thus, the total cobalt contribution of CoTTP|PPy|GaP samples is nearly identical to that estimated and previously reported[8c] for CoP-GaP samples (0.59 nmol cm^{-2}) in which no attempt was made to distinguish contributions from the front and back sides of the GaP wafer and thus represents an upper limit. However, XP spectroscopic analysis of the polished and unpolished faces of CoTTP|PPy|GaP samples prepared via UV illumination from the polished side of the wafer indicates that the surface cobalt concentration on the unpolished (nondirectly illuminated) side of the wafer is 33% lower than that of the polished (directly illuminated) side of the wafer, yielding a cobalt concentration of 0.39 ± 0.08 nmol cm^{-2} on the polished face. We note that the ratio of front to back side cobalt contributions is particularly useful when considering the per cobalt center PEC activity for hydrogen production given that the back side of the wafer is encased in epoxy and is not in contact with the electrolyte solution.

Photoelectrochemistry. Photoelectrochemical (PEC) experiments were performed in 0.1 M phosphate buffer (pH 7) under air mass (AM) 1.5 irradiation. A three-electrode configuration with GaP working electrodes (including GaP following buffered hydrofluoric acid treatment, polypyridine-modified GaP, and cobalt porphyrin modified GaP) was used in a cell containing a quartz window (Figure S17, see the Supporting Information for details). HER activity was calculated assuming unity Faradaic efficiency, although this was confirmed at only one point (0 V vs reversible hydrogen electrode (RHE)). Samples for post-PEC analysis were prepared using a customized three-electrode cell equipped with a quartz window and spring-loaded copper support to secure the GaP wafer, thus negating the need to encase the sample in epoxy (Figure S18). An indium−gallium eutectic was applied between the copper support and GaP sample. The electrodes were polarized at 0 V vs RHE for a minimum of 3 min under 1-sun illumination. Samples were rinsed with Mill-Q water and dried under vacuum before GATR-FTIR measurements. All PEC experiments were conducted under a continuous flow of 5% hydrogen in nitrogen.

Gas Chromatography. Gas chromatography (GC) was used to analyze aliquots of headspace gas taken from a sealed PEC cell both prior to and following 30 min of bulk electrolysis at 0 V vs RHE (see the Supporting Information for details). We note that the 93% Faradaic efficiency reported is likely a lower limit and does not correct for loss of hydrogen from the cell or during the sampling procedure.

RESULTS AND DISCUSSION

The cobalt porphyrin−polypyridine modified GaP semiconductors (CoTTP|PPy|GaP) described in this report are prepared using a two-step method (Figure 1) leveraging the UV-induced surface grafting chemistry of alkenes[11] to apply an initial thin-film polypyridine surface coating, followed by wet-chemical treatment to assemble the cobalt porphyrin units. During this process, freshly cleaned and etched GaP(100) wafers are placed in an argon-sparged solution of 4-vinylpyridine under shortwave UV illumination for 2 h before

DOI: 10.1021/acs.inorgchem.7b01509
Inorg. Chem. 2017, 56, 12178−12185

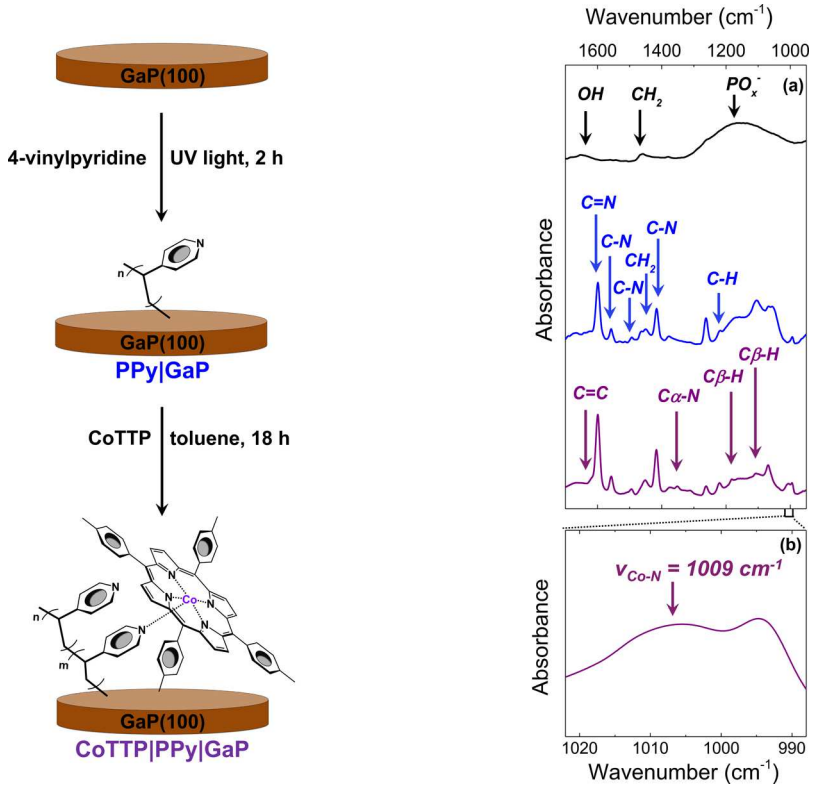

Figure 1. (left) Schematic representation of the synthetic method used to prepare the PPy|GaP and CoTTP|PPy|GaP samples. (right) GATR-FTIR absorbance spectra of (a) the 1700−950 cm^{-1} region of unfunctionalized GaP (black), PPy|GaP (blue), and CoTTP|PPy|GaP (purple), including an expanded plot of (b) the CoTTP|PPy|GaP spectrum, showing the in-plane porphyrin deformation mode labeled as ν_{Co-N} (where ν is the vibrational frequency).

removing and cleaning the functionalized wafers with successive solvent washes followed by drying under a stream of nitrogen (see the Experimental Section for details). The resulting polypyridine-modified substrates (PPy|GaP) are then exposed to a solution of CoTTP in toluene under an argon atmosphere for 18 h, forming CoTTP|PPy|GaP.

Analysis of CoTTP|PPy|GaP surfaces using grazing angle attenuated total reflection Fourier transform infrared (GATR-FTIR) spectroscopy confirms that cobalt centers of the porphyrin macrocycles coordinate to pyridyl nitrogen sites of the PPy graft (Figure 1). In addition to characteristic vibrational features associated with C−H and C−N vibrations of surface-grafted pyridyl units as well as the C_β−H, C_α−N, and C═C vibrations of the porphyrin macrocycle, a prominent absorption band is measured at 1009 cm^{-1}. Absorption bands appearing in the region from 1019 to 1004 cm^{-1} in the IR spectra of metalloporphyrins are ascribed to in-plane porphyrin deformations. This region is sensitive to both the elemental nature of the metal center and local coordination environment due to inductive and mesomeric effects.[12] The feature at 1009 cm^{-1} on CoTTP|PPy|GaP surfaces, labeled as ν_{Co-N} (Figure 1b), is particularly diagnostic of cobalt porphyrin complexes coordinated to an axial pyridyl unit[13] and thus provides structural information on the bonding motif of the surface-immobilized cobalt porphyrins.

Further information on the composition and structure of the modified surface, including film thickness, pyridyl site density, loading efficiency (defined here as the fraction of pyridyl sites coordinated to a cobalt center), and associated cobalt concentration per geometric area, is gained using complementary methods of ellipsometry, inductively coupled plasma mass spectrometry (ICP-MS), and X-ray photoelectron (XP) spectroscopy. Spectroscopic ellipsometry measurements of PPy|GaP surfaces are used to determine the film thickness and provide an estimate of the pyridyl site density. For the samples in this report, the obtained film thickness is 1.45 ± 0.17 nm. Given that the bulk polyvinylpyridine density (1.15 g cm^{-3}) is representative of the solvent-free film, the calculated pyridyl site density is 1.57 ± 0.18 nmol cm^{-2}.

ICP-MS measurements following acid digestion of PPy|GaP samples indicate that no significant cobalt is present. However, following attachment of cobalt porphyrin complexes, the Co surface concentration is estimated to be 0.39 ± 0.08 nmol cm^{-2} (see the Experimental Section for details). These measurements indicate that 25 ± 5% of the pyridyl units on the CoTTP|PPy|GaP surface are coordinated to a porphyrin cobalt center, equating to a total N/Co ratio of 4.1 ± 0.8. This ratio, as measured by ICP-MS and ellipsometry, is used to establish the N 1s background in XP spectra and assists in guiding the component fitting. We note that this method of combining information obtained from ICP-MS, ellipsometry, and XP spectroscopy is particularly useful in analyzing thin-film surface coatings on GaP as the N 1s spectrum contains background components arising from Ga 3d (Auger) LMM lines (Figure S8).[14]

As compared to XP spectra of unfunctionalized GaP or PPy|GaP samples, spectra of the CoTTP|PPy|GaP samples show additional Co and N contributions (Figures S7−S9). After applying the appropriate relative sensitivity factors, the N 1s to Co 2p spectral intensity ratio of 8.0 ± 0.8 yields a loading efficiency of 26 ± 6%, a value consistent with that determined by the ellipsometry and ICP-MS analysis. In addition, unlike

DOI: 10.1021/acs.inorgchem.7b01509
Inorg. Chem. 2017, 56, 12178−12185

the single component observed in the high-energy resolution N 1s spectra of PPy|GaP samples (Figure S8), spectra obtained using CoTTP|PPy|GaP samples can be deconvoluted into three components (Figure 2b). Based on the relative signal intensities

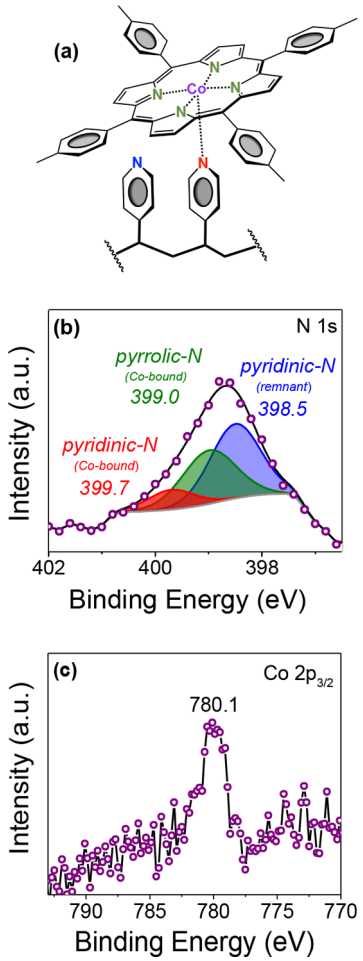

Figure 2. (a) Molecular structure of a CoTTP unit coordinated to polypyridine. (b) High-energy resolution XP spectrum of the N 1s region of CoTTP|PPy|GaP. Solid lines represent the background (gray), component (blue, green, and red), and overall (black) fits to the experimental data (circles). Shading indicates the component area assigned to remnant pyridinic nitrogens (blue), porphyrin pyrrolic nitrogens bound to cobalt centers (green), and pyridinic nitrogens bound to cobalt centers (red). (c) High-energy resolution XP spectrum of the Co $2p_{3/2}$ region of CoTTP|PPy|GaP.

and binding energies associated with these components, the contributions centered at 398.5, 399.0, and 399.7 eV are assigned to remnant pyridinic nitrogens of the surface graft, porphyrin pyrrolic nitrogens bound to cobalt centers, and pyridinic nitrogens bound to cobalt centers, respectively. Further, the ≈3:4:1 spectral intensity ratios associated with the three components are consistent with both the 4:1 ratio of cobalt-pyrollic to cobalt-pyridinic nitrogen centers anticipated for a cobalt porphyrin coordinated to a pyridyl unit and the 26 ± 6% loading efficiency determined by comparison of the total N 1s and Co 2p spectral intensity contributions. Finally, high-energy resolution XP spectra of the Co 2p region (Figure 2c and S9) show peaks centered at 780.1 eV ($2p_{3/2}$) and 795.3 eV ($2p_{1/2}$) with the anticipated 2:1 branching ratio and 15.2 eV splitting.[15] The Co $2p_{3/2}$ signal also shows satellite peaks at higher binding energies, consistent with the presence of cobalt species in the +2 oxidation state and the unpaired spin of the porphyrin cobalt center resting state.[16]

The PEC performance of custom-built working electrodes composed of CoTTP|PPy|GaP is assessed using three-electrode electrochemical techniques, including chronoamperometry (Figure 3a) and linear sweep voltammetry (Figure 3b), performed in buffered pH neutral aqueous conditions in the dark and under air mass 1.5 simulated solar illumination. Modification of GaP photocathodes with a cobalt porphyrin−polypyridyl surface coating results in a significant anodic shift of the open-circuit photovoltage (V_{oc}), moving from +0.57 ± 0.02 V vs RHE for the unmodified GaP electrodes to +0.65 ± 0.02 V vs RHE. We note that within the experimental error of the measurements the current density of −1.27 ± 0.04 mA cm^{-2} achieved for CoTTP|PPy|GaP samples polarized at 0 V vs RHE (i.e., at the H^+/H_2 equilibrium potential) is identical to that previously reported using GaP samples modified with a directly attached cobalt porphyrin monolayer (Figure S11).[8c] Thus, the intervening polypyridyl surface coating does not diminish the performance gains afforded by cobalt porphyrin surface modification yet reduces the synthetic efforts required for assembly. In addition, the saturating photocurrent shows a linear increase upon increasing illumination intensity, indicating that the PEC activity at 0 V vs RHE is in part limited by the photon flux (Figure S12). Characteristic of a photosynthetic assembly,[17] these results confirm that light, and no electrochemical forward biasing or use of sacrificial redox reagents, is the energy input required to generate the photocurrent.

Production of hydrogen is confirmed via gas chromatography analysis of headspace samples taken from a sealed PEC cell containing a CoTTP|PPy|GaP working electrode polarized at 0 V vs RHE under simulated solar illumination (Figure 3c). Under these conditions, hydrogen is produced at a rate of ≈10 μL min^{-1} cm^{-2} with a Faradaic efficiency of 93 ± 3%. Given the cobalt porphyrin surface concentration (0.39 ± 0.08 nmol cm^{-2}) determined by XP spectroscopy, ellipsometry, and ICP-MS, this equates to a HER activity per cobalt center of 17.6 H_2 molecules s^{-1} Co^{-1} (see the Experimental Section for details). During bulk electrolysis measurements, hydrogen bubbles accumulate on the electrode surface and diminish the surface area of the working electrode exposed to electrolyte, resulting in a decrease of current density over time (Figure S13). Removal of bubbles during or following PEC testing restores the current density to a value nearly identical to that achieved for a freshly prepared electrode. In addition, the observation of a prominent ν_{Co-N} in-plane porphyrin deformation mode in GATR-FTIR spectra of samples following bulk electrolysis (see the Experimental Section for details) indicates that cobalt porphyrins maintain their molecular integrity and coordination to pyridyl sites (Figure S14).

Additional insights regarding the performance gains afforded by cobalt porphyrin−polypyridyl surface modification come from analysis of the photovoltaic performance parameters derived from the voltammetry measurements, including those performed on control samples of working electrodes composed of unfunctionalized GaP and PPy|GaP (Table S2). Although CoTTP|PPy|GaP shows an enhanced V_{oc} compared to unmodified GaP, similar V_{oc} gains are obtained following only application of the thin-film polypyridyl surface coating (Figure S15). These results contrast to those reported using GaP semiconductors with thicker polymer coatings (on the order of ≈10 nm)[8e,f,q,r,s] where the V_{oc} instead decreases following

DOI: 10.1021/acs.inorgchem.7b01509
Inorg. Chem. 2017, 56, 12178−12185

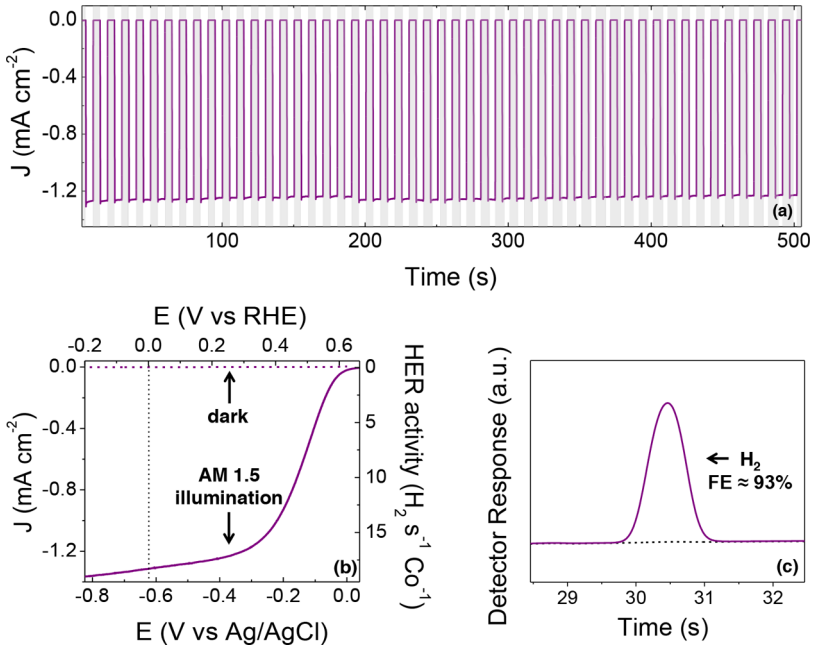

Figure 3. (a) Chronoamperogram of a CoTTP|PPy|GaP working electrode polarized at 0 V vs RHE under alternating (200 mHz) nonilluminated and illuminated (simulated AM 1.5) conditions. The gray shaded portions of the graph represent intervals under dark conditions. (b) Linear sweep voltammograms of CoTTP|PPy|GaP working electrodes recorded in the dark (dashed line) and under simulated 1-sun illumination (solid line). The dotted vertical line at 0 V vs RHE represents the equilibrium potential of the H^+/H_2 couple. The calculated HER activity per cobalt center is included on the right ordinate axis. (c) Gas chromatograms of a 5 mL aliquot of the headspace drawn from a sealed photoelectrochemical cell using a CoTTP|PPy|GaP working electrode polarized at 0 V vs RHE before (dashed line) and after (solid line) 30 min of illumination at 100 mW cm^{-2}. All measurements were performed using a three-electrode configuration in 0.1 M phosphate buffer (pH 7).

pyridyl group modification of the GaP surface. We speculate that this is in part due to a larger resistance and poorer ion conductivity associated with the thicker organic coatings.[18] Nonetheless, although the V_{oc} of the PPy|GaP and CoTTP|PPy|GaP electrodes is similar, the fill factor (ff) of the JV response under illumination nearly doubles following treatment with CoTTP, moving from 0.21 ± 0.08 for unfunctionalized GaP to 0.23 ± 0.07 for PPy|GaP, and further increasing to 0.39 ± 0.07 for CoTTP|PPy|GaP (Figure S15 and Table S2). Due to the steep increase in operating photocurrent densities that are produced by changes in ff, this can have a significant effect on performance in a photoelectrosynthetic cell.[3b]

CONCLUSION

In summary, surface-sensitive spectroscopic methods verify our synthetic efforts dedicated to construction of a hybrid composite material that structurally interfaces a cobalt porphyrin hydrogen evolution catalyst to a visible light-absorbing semiconductor using surface-attached pyridyl groups as molecular recognition sites. Complementary methods of ellipsometry, ICP-MS, and XP spectroscopy are used to quantify the surface cobalt concentrations and the fraction of pyridyl sites coordinated to cobalt centers. The synthetic methods used to obtain these assemblies demonstrate design principles for furthering hard-to-soft matter interface chemistry and set the stage to better understand the structure and function relationships of molecular-modified semiconductors. Key features of the construct reported here include the relative ease of synthetic preparation made possible by application of a thin-film organic coating that uses pyridyl groups to assemble cobalt porphyrins on a GaP semiconductor surface, yielding a hybrid photocathode that uses solar energy to drive reductive fuel-forming reactions in aqueous solutions without the use of organic acids or sacrificial chemical reductants. Thus, this work introduces a highly useful, yet easily accessible, motif for preparing and studying molecular-modified semiconductors. In order to elucidate the effect of the polymeric interface, studies using different bases and polymeric architectures to assemble CoTTP as well as other catalysts are underway.

ASSOCIATED CONTENT

Supporting Information

The Supporting Information is available free of charge on the ACS Publications website at DOI: 10.1021/acs.inorgchem.7b01509.

Synthesis and characterization of CoTTP, detailed experimental methods, FTIR data, XPS data, and electrochemical and photoelectrochemical data (PDF)

AUTHOR INFORMATION

Corresponding Author

*E-mail: gfmoore@asu.edu.

ORCID

G. F. Moore: 0000-0003-3369-9308

Funding

This material is based upon work supported by the National Science Foundation under Early Career Award 1653982. A.M.B. and B.L.W. are supported by an IGERT-SUN fellowship funded by the National Science Foundation (Award 1144616). D.K. acknowledges support from ASU LightWorks under the Technology and Research Initiative Fund.

Notes

The authors declare no competing financial interest.

DOI: 10.1021/acs.inorgchem.7b01509
Inorg. Chem. 2017, 56, 12178−12185

■ ACKNOWLEDGMENTS

The authors gratefully acknowledge Gwyneth Gordon in the W. M. Keck Foundation Laboratory for Environmental Biogeochemistry for assistance with ICP-MS measurements, Timothy Karcher in the LeRoy Eyring Center for Solid State Science for assistance with XPS data collection, and Marco Flores in the Electron Paramagnetic Resonance Facility for assistance with EPR data collection. NMR studies were performed using the Magnetic Resonance Research Center at Arizona State University.

■ REFERENCES

(1) (a) Faunce, T. A.; Lubitz, W.; Rutherford, A. W.; MacFarlane, D.; Moore, G. F.; Yang, P.; Nocera, D. G.; Moore, T. A.; Gregory, D. H.; Fukuzumi, S.; Yoon, K. B.; Armstrong, F. A.; Wasielewski, M. R.; Styring, S. Energy and Environment Policy Case for a Global Project on Artificial Photosynthesis. *Energy Environ. Sci.* **2013**, *6*, 695−698. (b) Faunce, T. A.; Styring, S.; Wasielewski, M. R.; Brudvig, G. W.; Rutherford, A. W.; Messinger, J.; Lee, A. F.; Hill, C. L.; DeGroot, H.; Fontecave, M.; MacFarlane, D. R.; Hankamer, B.; Nocera, D. G.; Tiede, D. M.; Dau, H.; Hillier, W.; Wang, L.; Amal, R. Artificial Photosynthesis as a Frontier Technology for Energy Sustainability. *Energy Environ. Sci.* **2013**, *6*, 1074−1076.

(2) (a) Nocera, D. G. Solar Fuels and Solar Chemicals Industry. *Acc. Chem. Res.* **2017**, *50*, 616−619. (b) Forbes, M. D. What We Talk About When We Talk About Light. *ACS Cent. Sci.* **2015**, *1*, 354. (c) Najafpour, M. M.; Barber, J.; Shen, J.-R.; Moore, G. F. Running on Sun. *Chem. World* **2012**, *43* (September). (d) Nozik, A. J.; Memming, R. Physical Chemistry of Semiconductor−Liquid Interfaces. *J. Phys. Chem.* **1996**, *100*, 13061−13078. (e) Bard, A.; Fox, M. A. Artificial Photosynthesis: Solar Splitting of Water to Hydrogen and Oxygen. *Acc. Chem. Res.* **1995**, *28*, 141−145.

(3) (a) Queyriaux, N.; Kaeffer, N.; Morozan, A.; Chavarot-Kerlidou, M.; Artero, V. Molecular Cathode and Photocathode Materials for Hydrogen Evolution in Photoelectrochemical Devices. *J. Photochem. Photobiol., C* **2015**, *25*, 90−105. (b) Walter, M. G.; Warren, E. L.; McKone, J. R.; Boettcher, S. W.; Mi, Q.; Santori, E. A.; Lewis, N. S. Solar Water Splitting Cells. *Chem. Rev.* **2010**, *110*, 6446−6473.

(4) (a) McKone, J. R.; Marinescu, S. C.; Brunschwig, B. S.; Winkler, J. R.; Gray, H. B. Earth-abundant Hydrogen Evolution Electrocatalysts. *Chem. Sci.* **2014**, *5*, 865−878. (b) Du, P.; Eisenberg, R. Catalysts Made of Earth-abundant Elements (Co, Ni, Fe) for Water Splitting: Recent Progress and Future Challenges. *Energy Environ. Sci.* **2012**, *5*, 6012−6021.

(5) (a) Armstrong, F. A.; Hirst, J. Reversibility and Efficiency in Electrocatalytic Energy Conversion and Lessons from Enzymes. *Proc. Natl. Acad. Sci. U. S. A.* **2011**, *108*, 14049−14054. (b) Armstrong, F. A.; Belsey, N. A.; Cracknell, J. A.; Goldet, G.; Parkin, A.; Reisner, E.; Vincent, K. A.; Wait, A. F. Dynamic Electrochemical Investigations of Hydrogen Oxidation and Production by Enzymes and Implications for Future Technology. *Chem. Soc. Rev.* **2009**, *38*, 36−51. (c) Albery, W. J.; Knowles, J. R. Evolution of Enzyme Function and the Development of Catalytic Efficiency. *Biochemistry* **1976**, *15*, 5631−5640.

(6) (a) Ginovska-Pangovska, B.; Dutta, A.; Reback, M. L.; Linehan, J. C.; Shaw, W. J. Beyond the Active Site: The Impact of the Outer Coordination Sphere on Electrocatalysts for Hydrogen Production and Oxidation. *Acc. Chem. Res.* **2014**, *47*, 2621−2630. (b) Hambourger, M.; Moore, G. F.; Kramer, D. M.; Gust, D.; Moore, A. L.; Moore, T. A. Biology and Technology for Photochemical Fuel Production. *Chem. Soc. Rev.* **2009**, *38*, 25−35. (c) Rutherford, A. W.; Moore, T. A. Mimicking Photosynthesis, But Just the Best Bits. *Nature* **2008**, *453*, 449.

(7) (a) Kaiser, B.; Fertig, D.; Ziegler, J.; Klett, J.; Hoch, S.; Jaegermann, W. Solar Hydrogen Generation with Wide-Band-Gap Semiconductors: GaP (100) Photoelectrodes and Surface Modification. *ChemPhysChem* **2012**, *13*, 3053−3060. (b) Liu, C.; Sun, J.; Tang, J.; Yang, P. Zn-doped p-Type Gallium Phosphide Nanowire Photocathodes from a Surfactant-free Solution Synthesis. *Nano Lett.* **2012**, *12*, 5407−5411. (c) Barton, E. E.; Rampulla, D. M.; Bocarsly, A. B. Selective Solar Driven Reduction of CO2 to Methanol Using a Catalyzed p-GaP Based Photoelectrochemical Cell. *J. Am. Chem. Soc.* **2008**, *130*, 6342−6344. (d) Gratzel, M. Photoelectrochemical Cells. *Nature* **2001**, *414*, 338−344. (e) Butler, M. A.; Ginley, D. S. P-Type GaP as a Semiconducting Photoelectrode. *J. Electrochem. Soc.* **1980**, *127*, 1273−1278. (f) Halmann, M. Photoelectrochemical Reduction of Aqueous Carbon Dioxide on p-Type Gallium Phosphide in Liquid Junction Solar Cells. *Nature* **1978**, *275*, 115−116. (g) Tomkiewicz, M.; Woodall, J. M. Photoassisted Electrolysis of Water by Visible Irradiation of a p-Type Gallium Phosphide Electrode. *Science* **1977**, *196*, 990−991. (h) Bockris, J. O. The Rate of the Photoelectrochemical Generation of Hydrogen at p-Type Semiconductors. *J. Electrochem. Soc.* **1977**, *124*, 1348−1355. (i) Ellis, A. B.; Bolts, J. M.; Kaiser, S. W.; Wrighton, M. S. Study of n-Type Gallium Arsenide- and Gallium Phosphide-based Photoelectrochemical Cells. Stabilization by Kinetic Control and Conversion of Optical Energy to Electricity. *J. Am. Chem. Soc.* **1977**, *99* (9), 2848−2854.

(8) (a) Wrighton, M. S. Surface Functionalization of Electrodes with Molecular Reagents. *Science* **1986**, *231*, 32−37. (b) Leung, J. J.; Warnan, J.; Nam, D. H.; Zhang, J. Z.; Willkomm, J.; Reisner, E. *Chem. Sci.* **2017**, *8*, 5172. (c) Khusnutdinova, D.; Beiler, A. M.; Wadsworth, B. L.; Jacob, S. I.; Moore, G. F. Metalloporphyrin-modified Semiconductors for Solar Fuel Production. *Chem. Sci.* **2017**, *8*, 253−259. (d) Wadsworth, B. L.; Beiler, A. M.; Khusnutdinova, D.; Jacob, S. I.; Moore, G. F. Electrocatalytic and Optical Properties of Cobaloxime Catalysts Immobilized at a Surface-Grafted Polymer Interface. *ACS Catal.* **2016**, *6*, 8048−8057. (e) Beiler, A. M.; Khusnutdinova, D.; Jacob, S. I.; Moore, G. F. Solar Hydrogen Production using Molecular Catalysts Immobilized on Gallium Phosphide (111)A and (111)B Polymer−Modified Photocathodes. *ACS Appl. Mater. Interfaces* **2016**, *8*, 10038−10047. (f) Beiler, A. M.; Khusnutdinova, D.; Jacob, S. I.; Moore, G. F. Chemistry at the Interface: Polymer−Functionalized GaP Semiconductors for Solar Hydrogen Production. *Ind. Eng. Chem. Res.* **2016**, *55*, 5306−5314. (g) Garner, L. E.; Steirer, K. X.; Young, J. L.; Anderson, N. C.; Miller, E. M.; Tinkham, J. S.; Deutsch, T. G.; Sellinger, A.; Turner, J. A.; Neale, N. R. Covalent Surface Modification of GaAs (100) Photocathodes for Water Splitting in Highly Acidic Electrolyte. *ChemSusChem* **2017**, *10*, 767−773. (h) Ilic, S.; Brown, E. S.; Xie, Y.; Maldonado, S.; Glusac, K. D. Sensitization of p-GaP with Monocationic Dyes: The Effect of Dye Excited-State Lifetime on Hole Injection Efficiencies. *J. Phys. Chem. C* **2016**, *120*, 3145−3155. (i) M. Ugeda, M.; Bradley, A. J.; Rodrigo, L.; Yu, M.; Liu, W.; Doak, P.; Riss, A.; Neaton, J. B.; Tilley, T. D.; Pérez, R.; Crommie, M. F. Covalent Functionalization of GaP (110) Surfaces via a Staudinger-Type Reaction with Perfluorophenyl Azide. *J. Phys. Chem. C* **2016**, *120*, 26448−26452. (j) Wilkins, S. J.; Paskova, T.; Reynolds, C. L.; Ivanisevic, A. Comparison of the Stability of Functionalized GaN and GaP. *ChemPhysChem* **2015**, *16*, 1687−1694. (k) Gu, J.; Yan, Y.; Young, J. L.; Steirer, K. X.; Neale, N. R.; Turner, J. A. Water Reduction by a p-GaInP2 Photoelectrode Stabilized by an Amorphous TiO2 Coating and a Molecular Cobalt Catalyst. *Nat. Mater.* **2015**, *15*, 456. (l) Seo, J.; Pekarek, R. T.; Rose, M. J. Photoelectrochemical Operation of a Surface-Bound, Nickel-Phosphine H2 Evolution Catalyst on p-Si(111): A Molecular Semiconductor|Catalyst Construct. *Chem. Commun.* **2015**, *51*, 13264−13267. (m) Downes, C. A.; Marinescu, S. C. Efficient Electrochemical and Photoelectrochemical H2 Production from Water by a Cobalt Dithiolene One-Dimensional Metal−Organic Surface. *J. Am. Chem. Soc.* **2015**, *137*, 13740−13743. (n) Cedeno, D.; Krawicz, A.; Moore, G. F. Hybrid Photocathodes for Solar Fuel Production: Coupling Molecular Fuel-production Catalysts with Solid-state Light Harvesting and Conversion Technologies. *Interface Focus* **2015**, *5*, 20140085. (o) Hu, S.; Shaner, M. R.; Beardslee, J. A.; Lichterman, M.; Brunschwig, B. S.; Lewis, N. S. Amorphous TiO2 Coatings Stabilize Si, GaAs, and GaP Photoanodes for Efficient Water Oxidation. *Science* **2014**, *344*, 1005−1009. (p) Lattimer, J. R. C.; Blakemore, J. D.; Sattler, W.; Gul, S.; Chatterjee, R.; Yachandra, V. K.; Yano, J.; Brunschwig, B. S.; Lewis, N.

DOI: 10.1021/acs.inorgchem.7b01509
Inorg. Chem. 2017, 56, 12178−12185

S.; Gray, H. B. Assembly, Characterization, and Electrochemical Properties of Immobilized Metal Bipyridyl Complexes on Silicon(111) Surfaces. *Dalton Trans.* **2014**, *43*, 15004−15012. (q) Krawicz, A.; Cedeno, D.; Moore, G. F. Energetics and Efficiency Analysis of a Cobaloxime-modified Semiconductor under Simulated Air Mass 1.5 Illumination. *Phys. Chem. Chem. Phys.* **2014**, *16*, 15818−15824. (r) Cedeno, D.; Krawicz, A.; Doak, P.; Yu, M.; Neaton, J. B.; Moore, G. F. Using Molecular Design to Control the Performance of Hydrogen-Producing Polymer-Brush-Modified Photocathodes. *J. Phys. Chem. Lett.* **2014**, *5*, 3222−3226. (s) Krawicz, A.; Yang, J.; Anzenberg, E.; Yano, J.; Sharp, I. D.; Moore, G. F. Photofunctional Construct that Interfaces Molecular Cobalt-based Catalysts for H2 Production to a Visible-light-absorbing Semiconductor. *J. Am. Chem. Soc.* **2013**, *135*, 11861−11868. (t) Moore, G. F.; Sharp, I. D. A Noble-metal-free Hydrogen Evolution Catalyst Grafted to Visible Light-absorbing Semiconductors. *J. Phys. Chem. Lett.* **2013**, *4*, 568−572. (u) Sun, Y.; Sun, J.; Long, J. R.; Yang, P.; Chang, C. J. Photocatalytic Generation of Hydrogen from Water Using a Cobalt Pentapyridine Complex in Combination with Molecular and Semiconductor Nanowire Photosensitizers. *Chem. Sci.* **2013**, *4*, 118−124. (v) Zhao, Y.; Swierk, J. R.; Megiatto, J. D.; Sherman, B.; Youngblood, W. J.; Qin, D.; Lentz, D. M.; Moore, A. L.; Moore, T. A.; Gust, D.; Mallouk, T. E. Improving the Efficiency of Water Splitting in Dye-sensitized Solar Cells by Using a Biomimetic Electron Transfer Mediator. *Proc. Natl. Acad. Sci. U. S. A.* **2012**, *109*, 15612−15616. (w) Hou, Y.; Abrams, B. L.; Vesborg, P. C. K.; Björketun, M. E.; Herbst, K.; Bech, L.; Setti, A. M.; Damsgaard, C. D.; Pedersen, T.; Hansen, O.; Rossmeisl, J.; Dahl, S.; Nørskov, J. K.; Chorkendorff, I. Bioinspired Molecular Co-catalysts Bonded to a Silicon Photocathode for Solar Hydrogen Evolution. *Nat. Mater.* **2011**, *10*, 434−438. (x) Mukherjee, J.; Peczonczyk, S.; Maldonado, S. Wet Chemical Functionalization of III−V Semiconductor Surfaces: Alkylation of Gallium Phosphide Using a Grignard Reaction Sequence. *Langmuir* **2010**, *26*, 10890−10896.

(9) (a) Auwärter, W.; Écija, D.; Klappenberger, F.; Barth, J. V. Porphyrins at Interfaces. *Nat. Chem.* **2015**, *7*, 105−120. (b) Weng, Z.; Jiang, J.; Wu, Y.; Wu, Z.; Guo, X.; Materna, K. L.; Liu, W.; Batista, V. S.; Brudvig, G. W.; Wang, H. Electrochemical CO2 Reduction to Hydrocarbons on a Heterogeneous Molecular Cu Catalyst in Aqueous Solution. *J. Am. Chem. Soc.* **2016**, *138*, 8076−8079. (c) Maurin, A.; Robert, M. Noncovalent Immobilization of a Molecular Iron-Based Electrocatalyst on Carbon Electrodes for Selective, Efficient CO2-to-CO Conversion in Water. *J. Am. Chem. Soc.* **2016**, *138*, 2492−2495. (d) Civic, M. R.; Dinolfo, P. H. Electrochemical Rectification of Redox Mediators Using Porphyrin-Based Molecular Multilayered Films on ITO Electrodes. *ACS Appl. Mater. Interfaces* **2016**, *8*, 20465−20473. (e) Lin, S.; Diercks, C. S.; Zhang, Y. B.; Kornienko, N.; Nichols, E. M.; Zhao, Y.; Paris, A. R.; Kim, D.; Yang, P.; Yaghi, O. M.; Chang, C. J. Covalent Organic Frameworks Comprising Cobalt Porphyrins for Catalytic CO2 Reduction in Water. *Science* **2015**, *349*, 1208−1213. (f) Oveisi, A. R.; Zhang, K.; Khorramabadi-Zad, A.; Farha, O. K.; Hupp, J. T. Stable and Catalytically Active Iron Porphyrin-based Porous Organic Polymer: Activity as Both a Redox and Lewis Acid Catalyst. *Sci. Rep.* **2015**, *5*, 10621. (g) Hod, I.; Sampson, M. D.; Deria, P.; Kubiak, C. P.; Farha, O. K.; Hupp, J. T. Fe-porphyrin-based Metal−organic Framework Films as High-surface Concentration, Heterogeneous Catalysts for Electrochemical Reduction of CO2. *ACS Catal.* **2015**, *5*, 6302−6309. (h) Costentin, C.; Robert, M.; Savéant, J. M. Current Issues in Molecular Catalysis Illustrated by Iron Porphyrins as Catalysts of the CO2-to-CO Electrochemical Conversion. *Acc. Chem. Res.* **2015**, *48*, 2996−3006. (i) Swierk, J. R.; Méndez-Hernández, D. D.; McCool, N. S.; Liddell, P.; Terazono, Y.; Pahk, I.; Tomlin, J. J.; Oster, N. V.; Moore, T. A.; Moore, A. L.; Gust, D. Metal-free Organic Sensitizers for Use in Water-splitting Dye-sensitized Photoelectrochemical Cells. *Proc. Natl. Acad. Sci. U. S. A.* **2015**, *112*, 1681−1686. (j) Costentin, C.; Drouet, S.; Robert, M.; Savéant, J. M. A Local Proton Source Enhances CO2 Electroreduction to CO by a Molecular Fe Catalyst. *Science* **2012**, *338*, 90−94. (k) Yao, S. A.; Ruther, R. E.; Zhang, L.; Franking, R. A.; Hamers, R. J.; Berry, J. F. Covalent Attachment of Catalyst Molecules to Conductive Diamond: CO2 Reduction Using "Smart" Electrodes. *J. Am. Chem. Soc.* **2012**, *134*, 15632−15635. (l) Kumar, B.; Llorente, M.; Froehlich, J.; Dang, T.; Sathrum, A.; Kubiak, C. P. Photochemical and Photoelectrochemical Reduction of CO2. *Annu. Rev. Phys. Chem.* **2012**, *63*, 541−569. (m) Lindsey, J. S.; Bocian, D. F. Molecules for Charge-based Information Storage. *Acc. Chem. Res.* **2011**, *44*, 638−650. (n) Moore, G. F.; Blakemore, J. D.; Milot, R. L.; Hull, J. F.; Song, H. E.; Cai, L.; Schmuttenmaer, C. A.; Crabtree, R. H.; Brudvig, G. W. A Visible Light Water-splitting Cell with a Photoanode Formed by Codeposition of a High-potential Porphyrin and an Iridium Water-oxidation Catalyst. *Energy Environ. Sci.* **2011**, *4*, 2389−2392. (o) Morozan, A.; Jousselme, B.; Palacin, S. Low-platinum and Platinum-free Catalysts for the Oxygen Reduction Reaction at Fuel Cell Cathodes. *Energy Environ. Sci.* **2011**, *4*, 1238−1254. (p) Losse, S.; Vos, J. G.; Rau, S. Catalytic Hydrogen Production at Cobalt Centres. *Coord. Chem. Rev.* **2010**, *254*, 2492−2504. (q) Morris, A. J.; Meyer, G. J.; Fujita, E. Molecular Approaches to the Photocatalytic Reduction of Carbon Dioxide for Solar Fuels. *Acc. Chem. Res.* **2009**, *42*, 1983−1994. (r) Savéant, J. M. Molecular Catalysis of Electrochemical Reactions. Mechanistic Aspects. *Chem. Rev.* **2008**, *108*, 2348−2378. (s) Moore, G. F.; Hambourger, M.; Gervaldo, M.; Poluektov, O. G.; Rajh, T.; Gust, D.; Moore, T. A.; Moore, A. L. A Bioinspired Construct that Mimics the Proton Coupled Electron Transfer Between P680●+ and the TyrZ-His190 Pair of Photosystem II. *J. Am. Chem. Soc.* **2008**, *130*, 10466−10467. (t) Collin, J. P.; Sauvage, J. P. Electrochemical Reduction of Carbon Dioxide Mediated by Molecular Catalysts. *Coord. Chem. Rev.* **1989**, *93*, 245−268. (u) Dhanasekaran, T.; Grodkowski, J.; Neta, P.; Hambright, P.; Fujita, E. P-terphenyl-sensitized Photoreduction of CO2 with Cobalt and Iron Porphyrins. Interaction between CO and Reduced Metalloporphyrins. *J. Phys. Chem. A* **1999**, *103*, 7742−7748. (v) Lexa, D.; Mispelter, J.; Savéant, J. M. Electroreductive Alkylation of Iron in Porphyrin Complexes. Electrochemical and Spectral Characteristics of Sigma-alkylironporphyrins. *J. Am. Chem. Soc.* **1981**, *103*, 6806−6812.

(10) (a) Lee, C. H.; Lindsey, J. S. One-Flask Synthesis of *Meso*-Substituted Dipyrromethanes and Their Application in the Synthesis of *Trans*-Substituted Porphyrin Building Blocks. *Tetrahedron* **1994**, *50*, 11427−11440. (b) Gao, G. Y.; Ruppel, J. V.; Allen, D. B.; Chen, Y.; Zhang, X. P. Synthesis of β-Functionalized Porphyrins via Palladium-Catalyzed Carbon - Heteroatom Bond Formations: Expedient Entry into β -Chiral Porphyrins. *J. Org. Chem.* **2007**, *72*, 9060−9066.

(11) (a) Wang, X.; Ruther, R. E.; Streifer, J. A.; Hamers, R. J. UV-induced Grafting of Alkenes to Silicon Surfaces: Photoemission Versus Excitons. *J. Am. Chem. Soc.* **2010**, *132*, 4048−4049. (b) Terry, J.; Linford, M. R.; Wigren, C.; Cao, R. Y.; Pianetta, P.; Chidsey, C. E. D. Alkyl-Terminated Si(111) Surfaces: A Core Level Photoelectron Spectroscopy Study. *J. Appl. Phys.* **1999**, *85*, 213−221. (c) Cicero, R. L.; Linford, M. R.; Chidsey, C. E. D. Photoreactivity of Unsaturated Compounds with Hydrogen-Terminated Silicon (111). *Langmuir* **2000**, *16*, 5688−5695. (d) Mischki, T. K.; Donkers, R. L.; Eves, B. J.; Lopinski, G. P.; Wayner, D. D. M. Reaction of Alkenes with Hydrogen-Terminated and Photooxidized Silicon Surfaces: A Comparison of Thermal and Photochemical Processes. *Langmuir* **2006**, *22*, 8359−8365. (e) Ruther, R. E.; Franking, R.; Huhn, A. M.; Gomez-Zayas, J.; Hamers, R. J. Formation of Smooth, Conformal Molecular Layers on ZnO Surfaces via Photochemical Grafting. *Langmuir* **2011**, *27*, 10604−10614. (f) Rosso, M.; Giesbers, M.; Arafat, A.; Schroen, K.; Zuilhof, H. Covalently Attached Organic Monolayers on SiC and Si_xN4 Surfaces: Formation Using UV Light at Room Temperature. *Langmuir* **2009**, *25*, 2172−2180. (g) Li, B.; Franking, R.; Landis, E. C.; Kim, H.; Hamers, R. J. Photochemical Grafting and Patterning of Biomolecular Layers onto TiO2 Thin Films. *ACS Appl. Mater. Interfaces* **2009**, *1*, 1013−1022. (h) Steenackers, M.; Sharp, I. D.; Larsson, K.; Hutter, N. A.; Stutzmann, M.; Jordan, R. Structured Polymer Brushes on Silicon Carbide. *Chem. Mater.* **2010**, *22*, 272−278.

(12) (a) Boucher, L. J.; Katz, J. J. The Infared Spectra of Metalloporphyrins (4000−160 cm-1). *J. Am. Chem. Soc.* **1967**, *89*, 1340−1345. (b) Kincaid, J.; Nakamoto, K. Vibrational Spectra of

DOI: 10.1021/acs.inorgchem.7b01509
Inorg. Chem. 2017, 56, 12178−12185

Transition Metal Complexes of Tetraphenylporphine. *J. Inorg. Nucl. Chem.* **1975**, *37*, 85−89.
(13) Wang, R.; Gao, B.; Jiao, W. A Novel Method for Immobilization of Co Tetraphenylporphyrins on P(4VP-co-St)/SiO 2: Efficient Catalysts for Aerobic Oxidation of Ethylbenzenes. *Appl. Surf. Sci.* **2009**, *255*, 4109−4113.
(14) Flores-Perez, R.; Zemlyanov, D. Y.; Ivanisevic, A. Quantitative Evaluation of Covalently Bound Molecules on GaP (100). *J. Phys. Chem. C* **2008**, *112*, 2147−2155.
(15) (a) Chuang, T. J.; Brundle, C. R.; Rice, D. W. X-ray Photoemission Spectra of Cobalt Oxides and Cobalt Oxide Surfaces. *Surf. Sci.* **1976**, *59*, 413−429. (b) Dillard, J. G.; Schenck, C. V.; Koppelman, M. H. Surface Chemistry of Cobalt in Calcined Cobalt-Kaolinite Materials. *Clays Clay Miner.* **1983**, *31*, 69−72.
(16) Borod'Ko, Y. G.; Vetchinkin, S. I.; Zimont, S. L.; Ivleva, I. N.; Shul'Ga, Y. M. Nature of Satellites in X-ray Photoelectron Spectra XPS of Paramagnetic Cobalt (II) Compounds. *Chem. Phys. Lett.* **1976**, *42*, 264−267.
(17) Osterloh, F. E. Photocatalysis versus Photosynthesis: A Sensitivity Analysis of Devices for Solar Energy Conversion and Chemical Transformations. *ACS Energy Lett.* **2017**, *2*, 445−453.
(18) (a) Jeong, H.; Kang, M. J.; Jung, H.; Kang, Y. S. Electrochemical CO_2 Reduction with Low Overpotential by a Poly(4-vinylpyridine) Electrode for Application to Artificial Photosynthesis. *Faraday Discuss.* **2017**, *198*, 409. (b) Hurrell, H. C.; Abruna, H. D. Redox Conduction in Electropolymerized Films of Transition-metal Complexes of Osmium, Ruthenium, Iron, and Cobalt. *Inorg. Chem.* **1990**, *29*, 736−741. (c) Andrieux, C. P.; Dumas-Bouchiat, J. M.; Savéant, J. M. Catalysis of Electrochemical Reactions at Redox Polymer Electrodes: Kinetic Model for Stationary Voltammetric Techniques. *J. Electroanal. Chem. Interfacial Electrochem.* **1982**, *131*, 1−35.

DOI: 10.1021/acs.inorgchem.7b01509
Inorg. Chem. 2017, 56, 12178−12185